Desalination and Water Treatment
www.deswater.com

doi: 10.5004/dwt.2023.29317

285 (2023) 298–304
February

Degradation of Reactive Black 5 by ultrasound-activated persulfate process: kinetics, mineralization, and by-products

Paul Anthony[a], Şifa Doğan[b,*]

[a]*Institute of Graduate Studies and Research, Bioengineering Ph.D. Program, Cyprus International University, Haspolat, Nicosia, North Cyprus, Mersin 10, Turkey*
[b]*Engineering Faculty, Environmental Engineering Program, Cyprus International University, Haspolat, Nicosia, Mersin 10, Turkey, email: sdogan@ciu.edu.tr*

Received 25 July 2022; Accepted 18 January 2023

ABSTRACT

The synergetic effect of medium-high frequency ultrasound (575–861–1,141 kHz) was tested to improve the removal efficiency and rate of a model recalcitrant compound namely Reactive Black 5 (RB5) from water. The optimum ultrasonic frequency and power conditions were found as 575 kHz and 60 W. Ultrasound was combined with various doses of persulfate (PS) and when combined with a 1:1,000 RB5:PS ratio 88% removal was achieved after 90 min under acidic conditions. Addition of Fe^{2+} to US:PS process speeded up the reaction and the reaction rate was increased from 0.0215 to 0.0541 min^{-1} with a 1:1,000:1 RB5:PS:Fe^{2+} ratio. PS consumption is greatest when the PS:Fe^{2+} process is applied (18%) however complete elimination of RB5 was not achieved until 90 min. On the other hand, PS consumption by US:PS:Fe^{2+} process was lesser and more stable within 60 and 90 min where almost complete elimination was achieved. Synergy index of US:PS:Fe^{2+} process was found 0.96 confirming that the process is a promising technique with lower consumption of oxidant and faster reaction rates. The optimum US:PS:Fe^{2+} process resulted in 67% NPOC removal after 90 min and the identified by-products by LCMS spectra were also listed. Treated samples showed severe toxicity on gram-negative bacteria namely *Escherichia coli* compare to gram-positive *Bacillus subtilis*.

Keywords: Textile wastewater treatment; Persulfate oxidation; Ultrasonic irradiation; Reactive Black 5; Mineralization

1. Introduction

The use of synthetic dyes has increased the level of water pollution which poses a great threat to the environment. Dyes in water are undesirable due to their coloration, suspended solids, high level of biochemical oxygen demand values, chemical oxygen demand values, acidity, basicity, and other soluble substances and their impact on the ecology and environment due to their toxic, mutagenic, and carcinogenic nature [1]. Color removal from textile wastewater has attracted huge attention in the last two decades, not because of its potential toxicity but mostly due to its presence in waters. In particular, Reactive Black 5 (RB5) which belongs to the class of textile azo dyes which make up about 70% of all dyes produced globally and make up 50% of the total global dye demand is widely used in the textile industries [2]. To remove these dyes from water, various physical/chemical processes are required. In this regard, advanced oxidation processes (AOPs) were found to be a more promising technology for the degradation of recalcitrant organic pollutants. According to numerous studies carried out, hydroxyl radical (•OH) based AOPs showed a high efficiency in the degrading of emerging pollutants [3]. Recently, an investigation into the potential of sulfate radical (SO_4^{-}) in the degradation of emerging pollutants presented an obvious advantage to hydroxyl radical

* Corresponding author.

owing to its high oxidation potential (E^0 = 2.5–3.1 V), as compared with •OH (E^0 = 2.8 V), and it being nonselective to the pollutants [4]. Also, SO_4^- has a longer lifetime (30–40 μs) than •OH (0.02 μs) which permits the degradation of more organic contamination by sulfate radicals [5]. Moreover, persulfate oxidants are convenient to use due to their high solubility. Persulfate-based AOPs have been widely applied in environmental remediation for degrading contaminants and are generated using various activation methods to separate the O–O bond of PS [6–13]. In recent years, numerous kinds of organic analytes including pesticides, dyes, and pharmaceuticals, have emerged and related research on the activation methods, the mechanism, and the application have been performed. Numerous activation methods including microwave [14], ultraviolent [15], transition metals [16], heat [17], alkalis carbon materials [18], and nanomaterials [19] have all been explored in the past decades. Despite all of these, ultrasound activation, an emerging method has been found to be more effective and is currently gaining huge momentum, especially in the last 5 y. AOPs can be defined as a "Green Process" as a result of the in-situ production of radicals. Among AOPs, ultrasonic irradiation causes the collapse of cavitation bubbles which results in enormous heat release which can be used to activate the persulfate ions to generate additional radicals in aqueous matrices. Also, US irradiation helps to increase mass transfer and chemical reaction rates, cleans the solid surfaces, and enhances catalytic activities [20,21]. For those characteristics of ultrasound, its application on the activation of persulfate is a promising process to study.

In literature, the performance of US and PS combination with or without solid catalysts were tested under low-frequency conditions such as 20, 40, 60, and 130 kHz [22–35]. In this study, RB5 was selected as a recalcitrant pollutant where few studies [36,37] exist to reveal US performance for its removal. There is a lack of information in the literature about the medium-high frequency ultrasound activation of persulfate and its investigation is important because the medium-high frequency ultrasound is targeted to non-volatile and moderately-low water soluble water pollutants. This study aims to investigate the removal and mineralization of RB5 under high-frequency ultrasonic irradiation (575–861–1,141 kHz) and at various molar ratios of RB5:PS (1:100, 1:500 and 1:1,000) and three different pH conditions (3, 7, 10) to reveal to lack of information exist in the literature. A complete study of reaction kinetics, mineralization rate, and by-product formation was investigated.

2. Materials and methods

2.1. Reagents and materials

Azo dye also known as Remazol Black B, RB5 (65% dye content), and chloramphenicol, 30 μg (C-30) were purchased from Sigma-Aldrich (Germany). Sodium hydroxide (NaOH) pure pellets, sulfuric acid, (95%–97%), ferrous sulfate ($FeSO_4$), and potassium peroxodisulfate ($K_2O_8S_2$), sodium hydrogen carbonate ($NaHCO_3$), potassium iodide (KI), hydrochloric acid (37% HCl), methanol and nutrient agar purchased from Merck (Germany). Deionized water was produced using Sartorius (Arium 61631) system. C_{18} SPE cartridges were obtained from Cayman Chemical Company (USA). *Escherichia coli* and *Bacillus subtilis* were supplied from Biomerieux LyfoCults (France).

2.2. Methods

The ultrasonic system was purchased from Meinhardt Ultraschalltechnik Company (Germany) which is composed of US generator (575–861–1,141 kHz) coupled with a double-jacked glass reactor connected to a titanium plate type of transducer. The concentration of RB5 was measured using a Shimadzu UV-2450 UV-Vis spectrophotometer (Japan) to obtain absorbance values at 579 nm. Mineralization was measured by the NPOC method using TOC-V_{CPN} Total Organic Carbon Analyzer. 0.5% 5 M HCl was sparged for 2 min, and 50 μL sample was injected for analysis. A calibration curve was prepared 0–10 mg·L^{-1}. By-product analysis was conducted by Shimadzu liquid chromatography coupled with applied bioscience MSMS detector. Samples after solid phase extraction were introduced to the LCMS system to scan mass range between 50–500 amu. Solid phase extraction was done prior to LCMS analysis which was as follows: C18 cartridges were conditioned with 5 mL methanol, washed with 5 mL deionized water, and 100 mL were passed through the cartridge and eluted in 5 mL methanol. Persulfate concentration was measured by the spectrophotometric method described previously [38].

Toxicity tests were performed by disk diffusion antibiotic sensitivity test also known as Kirby–Bauer Test [39]. Two microorganisms *Escherichia coli* (gram-) and *Bacillus subtilis* (gram+) were inoculated in a nutrient agar medium. As a control chloramphenicol, 30 μg (C-30) antibiotic disc was used. The zone of inhibition which is a circular area around the spot of the antibiotic disc and treated sample was measured.

Ultrasonic power measurement was done by the calorimetric method [40]. US reactor was operated at 575 kHz and 60 W by placing 250 mL deionized water in the reactor and the temperature of the deionized water within 1 for 30 min was measured by a thermometer and plotted against time. The power diffused into the system has been calculated by Eq. (1) where; P_d is diffused power into the system, dT/dt is temperature rise (°C/min) which is the linear slope of the parabolic curves which was created by plotting temperature readings vs., C_p is the heat capacity of water (4.184 J/g·°C) and M is the mass of water inside the reactor which was equal to 250 g as the density of water is 1 g/mL. The diffused power into the system was calculated as 14.6 under 60 W power conditions.

$$P_d = \frac{dT}{dt} \times C_p \times M \tag{1}$$

2.3. Experimental set-up

50 mg·L^{-1} RB5 dye solution was prepared by dissolving 0.05 g in 1 L pure water. Three different pH range (3, 7, and 10) was tested to reveal the pH effect, and the adjustment was done by 1% NaOH and 1% HCl. Removal of RB5 was tested by following advanced oxidation processes: Ultrasound alone at three different frequencies (575–861–1,141 kHz) at 60 W; ultrasound combined with persulfate

with molar ratios of 1:100, 1:500, 1;1,000; persulfate combined with Fe^{2+} with molar ratios of 1,000:0.25, 1,000:0.5 and 1,000:1 and finally ultrasound combined with persulfate and Fe^{2+} with molar ratios of 1:1,000:0.25, 1:1,000:0.5 and 1:1,000:1. 250 mL RB5 dye sample at room temperature and allowed to undergo reaction for 90 min. For concentration measurements, samples were withdrawn at time intervals of 0, 1, 5, 10, 30, 60, and 90 min. Persulfate concentration was monitored at 0, 60, and 90 min; mineralization was measured at 0 and 90 min.

3. Results

The efficiency of ultrasonic irradiation was tested by 575–861–1,141 kHz frequencies and 3–7–10 pH range. It was observed that the maximum removal (25%) occurred at 575 kHz frequency at pH 3 (Fig. 1).

Ultrasonic irradiation at an optimum frequency (575 kHz) was combined with persulfate. The molar ratio between RB5 and persulfate was selected as 1:100, 1:500, 1:1,000. The results showed that the highest RB5:persulfate ratio (1:1,000) resulted in the maximum concentration removal. Compare to the removal percentage by US alone and PS alone (1:1,000) which were 25% and 23%, respectively, the removal was increased up to 88% after 90 min (Fig. 2). Ultrasound alone has a limited capacity to cause efficient elimination of pollutants and 1%–20% removal efficiency was reported previously [1,12]. Ultrasound plays a vital role in synergetic action rather than applied alone as it enhances the mass transfer reaction of constituents in the solution, activates persulfate molecules to generate sulfate radicals, and additionally generates hydroxyl radicals by water sonolysis.

The RB5 removal was faster under acidic conditions compared to neutral and alkaline conditions. Fig. 3 shows the pH effect at 1:1,000 RB5:PS molar ratio and the reaction rate constant at pH 3 was found as 0.031 min^{-1}. The molecule becomes more hydrophobic due to the protonation of the negatively charged $–SO_3–$ group under acidic conditions [36] and the increased hydrophobicity might cause faster degradation of the molecule when exposed to high-frequency ultrasound. In addition, previously sulfate radicals were found dominant under acidic conditions [41,42] which can explain the higher efficiency of the persulfate process observed at pH 3.

US:PS has been combined with various doses of Fe^{2+}. The molar ratio between RB5:PS: Fe^{2+} was adjusted to 1:1,000:0.25, 1:1,000:0.5, and 1:1,000:1. Degradation curves (Fig. 4) showed when Fe^{2+} dose increased from 1:1,000:0.25 to 1:1,000:0.5 the removal of RB5 increased drastically whereas there was a slight difference between 0.5 to 1 but yet 1:1,000:1 was significantly the ratio where highest removal was observed. In addition, degradation curves best fitted to first-order kinetics and the observed reaction rate constants are shown in Fig. 4. 1:1,000:1 molar ratio has the highest reaction rate constant.

The synergetic effect of US:PS:Fe^{2+} combination is obvious where after 60 min 96% removal was achieved by the process. It was also observed that PS:Fe^{2+} showed limited capacity compared to US:PS:Fe^{2+} to remove the RB5 from water that 88% concentration removal was reported after 90 min (Fig. 5). In addition, the kinetic analysis revealed that the observed reaction rate for PS:Fe^{2+} process was 0.0215 min^{-1}

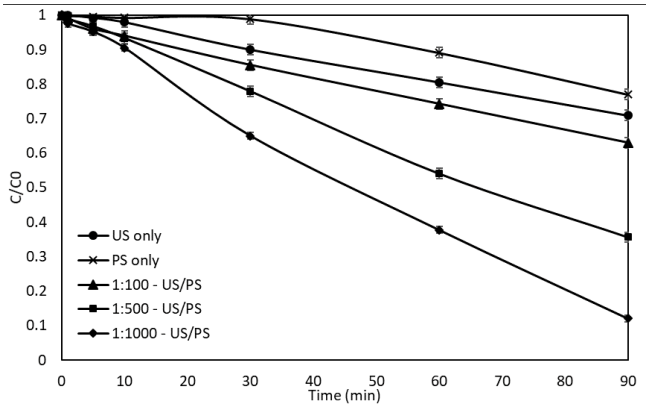

Fig. 2. US irradiation combined with PS under various RB5:PS molar ratio (US frequency = 575 kHz, power = 60 W, pH = 3, [RB5] = 50 $mg·L^{-1}$).

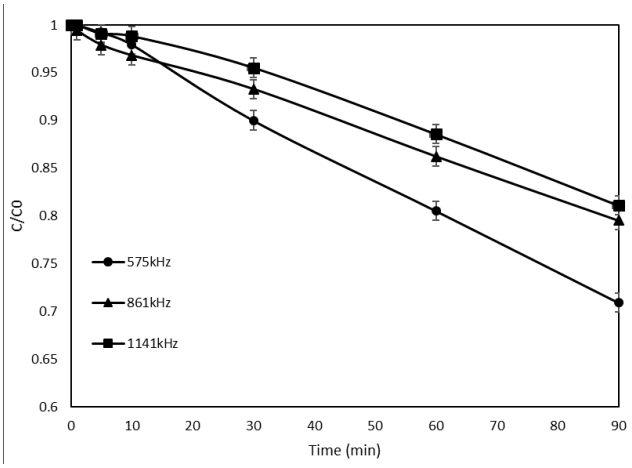

Fig. 1. Effect of ultrasonic frequency for RB5 removal [RB5] = 50 $mg·L^{-1}$, pH = 3, P = 60 W.

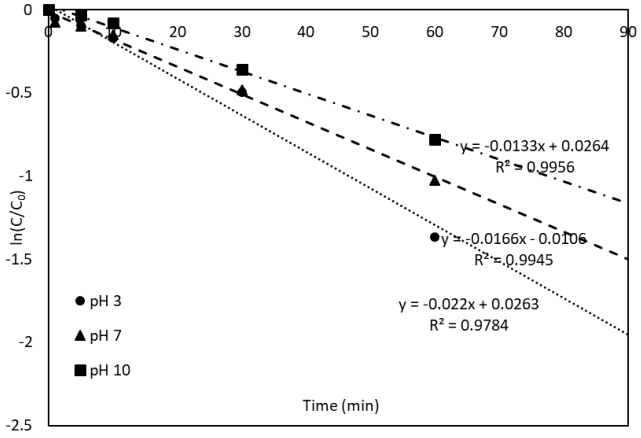

Fig. 3. Removal kinetics of RB5 under various pH conditions ([RB5] = 50 $mg·L^{-1}$, RB5:PS molar ratio is 1:1,000, US frequency = 575 kHz, P = 60 W).

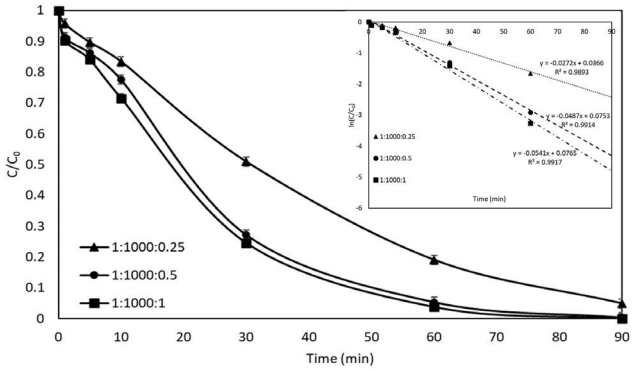

Fig. 4. Removal of RB5 by US:PS:Fe^{2+} process at 575 kHz 60 W and pH 3 conditions and the observed reaction rate constants.

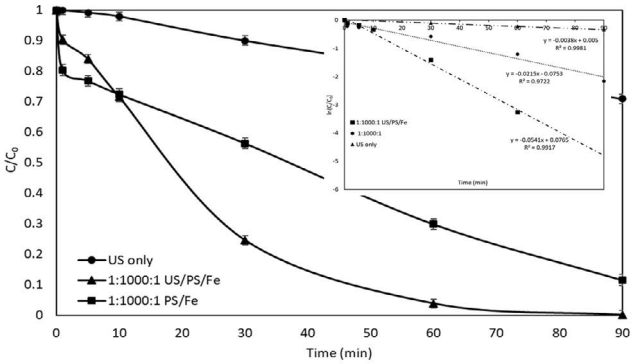

Fig. 5. Comparison of the efficiency of US:PS:Fe^{2+} and PS:Fe^{2+} process for the removal of RB5 and the observed reaction rate constants.

which is smaller than the constant calculated for US:PS:Fe^{2+} process which was 0.0541 min^{-1} (Fig. 5).

The efficiency of the combined US:PS:Fe^{2+} process was also expressed by synergy index *S*, which was calculated by Eq. (2) [42]. It can be used to explain the synergetic actions in combined systems from an engineering point of view such as working with lower concentrations of oxidants and obtaining faster process efficiencies by comparing the observed reaction rate constants. In this study, the observed first-order kinetic constants and the calculated synergetic index are given in Table 1. As the index was found greater than 0, it can be concluded that US:PS:Fe^{2+} process caused a synergetic action. This is also confirmed by lower PS consumption and higher absorbance removal within 60 min.

$$S = \frac{k_{\text{combined}}}{\sum_i^n k_i} \tag{2}$$

According to the literature, the most abundant anions found in real textile effluents were SO_4^{2-} and Cl^- [43]. In this study, the optimum US:PS:Fe^{2+} process was conducted in the presence of 1,000 mg·L^{-1} Cl^-. It was observed that the presence of Cl^- reduced the observed first-order reaction rate to 0.0248 min^{-1} (Fig. 6). It has been also previously reported that the concentration of chloride at critical levels can react and consume the radicals in the system thus resulting decrease in removal rates [43].

PS residual measurements are given in Table 2. PS consumption is greatest when PS:Fe^{2+} process is applied (18%) and the removal of RB5 continues until 90 min (88% absorbance decrease). On the other hand, US:PS:Fe^{2+} caused faster pollutant elimination where after 60 min there was no considerable amount of RB5 remaining. Previously, it was reported that [44] when the concentration of pollutant is high the greater the process parameters used or vice versa. Here, the production of sulfate radicals lowered as the US:PS:Fe^{2+} caused RB5 elimination. Also, mineralization has started and in the system various by-products are present. Further investigation in US:PS:Fe^{2+} system should be done to examine radical mechanisms within this system.

Mineralization was measured for the optimum US:PS, PS:Fe^{2+}, and US:PS:Fe^{2+} process. No significant mineralization

Table 1
The observed first-order reaction rate constants (*k*, min^{-1}) and synergy index (*S*)

Process	US	US:PS	PS:Fe^{2+}	US:PS:Fe^{2+}
k (min^{-1})	0.0038	0.0310	0.0215	0.0541
S	–	–	–	0.96

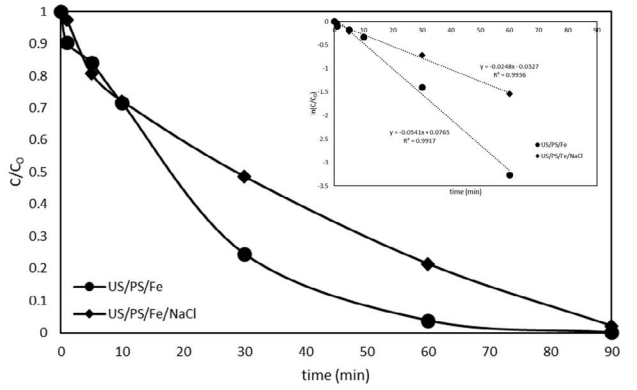

Fig. 6. Degradation curves and the observed reaction rate constants by US:PS:Fe^{2+} process in the presence and absence of Cl^-.

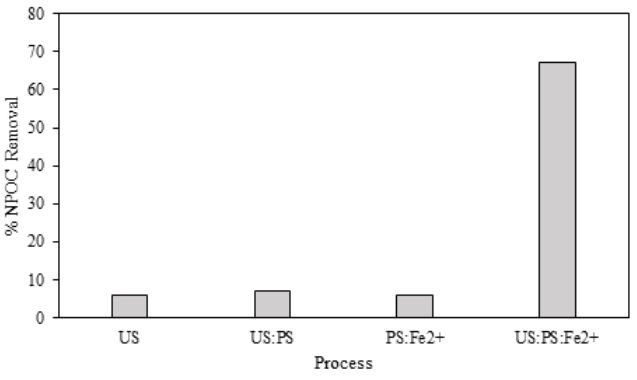

Fig. 7. NPOC removal by US, US:PS, PS:Fe^{2+}, and US:PS:Fe^{2+} processes.

was recorded during US:PS and PS:Fe^{2+} (0%–7%) processes however US:PS:Fe^{2+} combination resulted in 67% NPOC removal after 90 min. Mineralization results are shown in Fig. 7.

Figs. 8–10 shows LCMS spectra after 90 min of treatments of RB5 samples with US:PS, PS:Fe^{2+}, and US:PS:Fe^{2+}. 88%–100% decolorization of RB5 was achieved by these processes within 90 min. Decolorization is caused by the cleavage of

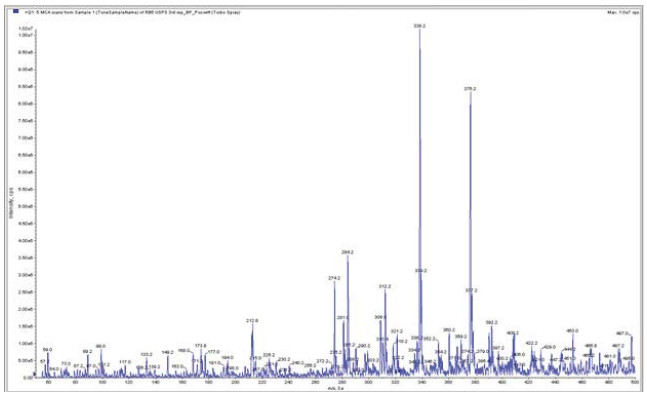

Fig. 8. LCMS spectrum after 90 min of US:PS treatment.

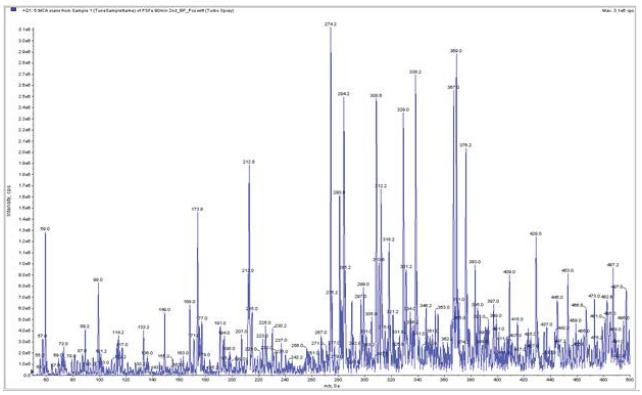

Fig. 9. LCMS spectrum after 90 min of PS:Fe^{2+} treatment.

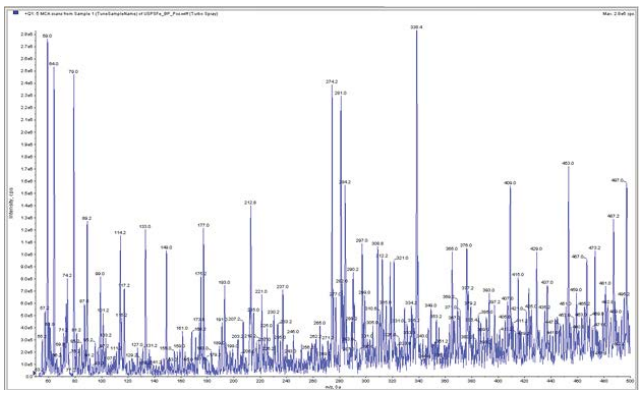

Fig. 10. LCMS spectrum after 90 min of US:PS:Fe^{2+} treatment.

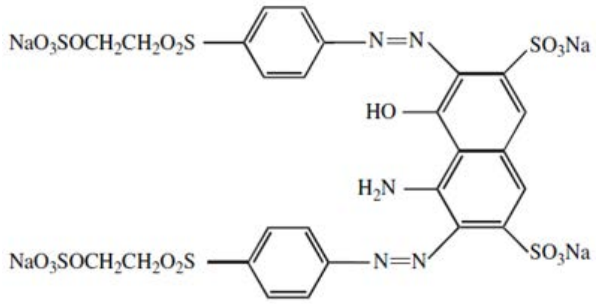

Fig. 11. Reactive Black 5 chemical structure.

Table 2
Persulfate consumption after US:PS, PF:Fe^{2+} and US:PS:Fe^{2+} processes

Time (min)	$[PS]_t/[PS]_0$		
	US:PS	PS:Fe^{2+}	US:PS:Fe^{2+}
0	1	1	1
60	0.96	0.87	0.92
90	0.89	0.82	0.91

Fig. 12. Toxicity test results after US:PS:Fe^{2+} process.

N=N double bonds of the molecule (Fig. 11) and the possible expected by-products are 349 and 280 amu [45–48]. In this study, 271, 281, and 284 amu were observed in LCMS spectra which can be attributed to the 1-sulphonic,2-(4-aminobenzenesulphonyl ethanol). Also, the other most abundant peaks were 369, 338, 367, and 376 amu which can be formed after the extraction of some ions from the 1,2,7-triamino-8-hydrox y-3,6-naphthalinedisulfonate molecule.

It was observed that treated samples have severe adverse effects *Escherichia coli* compared to *Bacillus subtilis* (Fig. 12). Further investigations should be made to remove excess oxidant persulfate from the system after treatment which might be responsible for the toxicity observed.

4. Conclusion

In this study, ultrasound has shown a significant synergetic effect on improving the traditional PS:Fe^{2+} process. Under 575 kHz frequency and 60 W power conditions and at 1:1,000:1 Dye:PS:Fe^{2+} molar ratio, 96% color removal within 60 min was achieved by US:PS:Fe^{2+} process at acidic conditions. PS consumption is greatest when US:PS:Fe^{2+} process is applied (22%). On the other hand, PS:Fe^{2+} and US:PS have almost the same PS consumption. It was obvious that the presence of US decomposed PS more efficiently into sulfate and other radicals in the presence of Fe^{2+}. The combined effect of ultrasound with PS:Fe^{2+} process resulted in faster removal as the reaction rate increased 2.5 folds from 0.0215 min^{-1} (PS:Fe^{2+}) to 0.0541 min^{-1} and 67% NPOC removal after 90 min. However, the presence of selected major matrix constituent 1,000 $mg{\cdot}L^{-1}$ Cl^- ion adversely affected the removal process as the reaction rate decreased to 0.0248 min^{-1}, and 98% color removal was achieved within 90 min.

The most abundant observed by-products by LCMS spectra have 271, 281, 284, 369, 338, 367, and 376 m/z ratio and their mass were found very close to the products possibly occurring after cleavage of N=N double bond as complete color removal was also observed. Toxicity tests revealed that the treated sample has a serious effect on gram-negative organism *Escherichia coli* compared to gram-positive *Bacillus subtilis*. Increasing the reaction and removing the excess amount of persulfate oxidant and sulfate ions should be further investigated to reduce the toxicity.

References

[1] S. Wang, N. Zhou, Removal of carbamazepine from aqueous solution using sono-activated persulfate process, Ultrason. Sonochem., 29 (2016) 156–162.

[2] C. Schumacher, More Challenges in the Greenpeace Detox Campaign, 2012. Available at: http://blog.stepchange-innovations.com/2012/11/more-challenges-in-the-greenpeace-detox-campaign/ (Accessed 26 January 2016).

[3] Y. Zhang, Y. Zhuang, J. Geng, H. Ren, K. Xu, L. Ding, Reduction of antibiotic resistance genes in municipal wastewater effluent by advanced oxidation processes, Sci. Total Environ., 550 (2016) 184–191.

[4] I. Hussain, Y. Zhang, S. Huang, Degradation of aniline with zero-valent iron as an activator of persulfate in aqueous solution, RSC Adv., 4 (2014) 3502–3511.

[5] F. Ghanbari, M. Moradi, F. Gohari, Degradation of 2,4,6-trichlorophenol in aqueous solutions using peroxymonosulfate/activated carbon/UV process via sulfate and hydroxyl radicals, J. Water Process Eng., 9 (2016) 22–28.

[6] L.W. Matzek, K.E. Carter, Activated persulfate for organic chemical degradation: a review, Chemosphere, 151 (2016) 178–188.

[7] T. Olmez-Hanci, I. Arslan-Alaton, Comparison of sulfate and hydroxyl radical based advanced oxidation of phenol, Chem. Eng. J., 224 (2013) 10–16.

[8] N.S. Shah, X. He, J.A. Khan, H.M. Khan, D.L. Boccelli, D.D. Dionysiou, Comparative studies of various iron-mediated oxidative systems for the photochemical degradation of endosulfan in aqueous solution, J. Photochem. Photobiol., 306 (2015) 80–86.

[9] T. Liu, B. Yao, Z. Luo, W. Li, C. Li, Z. Ye, X. Gong, J. Yang, Y. Zhou, Applications and influencing factors of the biochar-persulfate based advanced oxidation processes for the remediation of groundwater and soil contaminated with organic compounds, Sci. Total Environ., 836 (2022) 155421, doi: 10.1016/j.scitotenv.2022.155421.

[10] H. Ferkous, S. Merouani, O. Hamdaoui, C. Petrier, Persulfate-enhanced sonochemical degradation of naphthol blue-black in water: evidence of sulfate radical formation, Ultrason. Sonochem., 34 (2017) 580–587.

[11] E. Kattel, B. Kaur, M. Trapido, N. Dulova, Persulfate-based photodegradation of a beta-lactam antibiotic amoxicillin in various water matrices, Environ. Technol., 41 (2020) 202–210.

[12] E. Kattel, M. Trapido, N. Dulova, Oxidative degradation of emerging micropollutant acesulfame in aqueous matrices by UVA-induced H_2O_2/Fe^{2+} and $S_2O_8^{2-}/Fe^{2+}$ processes, Chemosphere, 171 (2017) 528–536.

[13] P. Gayathri, R.P.J. Dorathi, K. Palanivelu, Sonochemical degradation of textile dyes in aqueous solution using sulphate radicals activated by immobilized cobalt ions, Ultrason. Sonochem., 17 (2010) 566–571.

[14] F. Wang, C. Wu, Q. Li, Treatment of refractory organics in strongly alkaline dinitrodiazophenol wastewater with microwave irradiation-activated persulfate, Chemosphere, 254 (2020) 126773, doi: 10.1016/j.chemosphere.2020.126773.

[15] L. He, H. Chen, L. Wu, Z. Zhang, Y. Ma, J. Zhu, J. Liu, X. Yan, H. Li, L. Yang, Synergistic heat/UV activated persulfate for the treatment of nanofiltration concentrated leachate, Ecotoxicol. Environ. Saf., 208 (2021) 111522, doi: 10.1016/j.ecoenv.2020.111522.

[16] O. Pourehie, J. Saien, Treatment of real petroleum refinery wastewater with alternative ferrous-assisted UV/persulfate homogeneous processes, Desal. Water Treat., 142 (2019) 140–147.

[17] O.A. Andrew, S. Pirgalıoğlu, Ş. Doğan, Heat activated persulfate oxidation of Reactive Black 5, Desal. Water Treat., 177 (2020) 393–399.

[18] Y. Guo, K. Xuan, C. Pu, Y. Li, Y. Huang, Y. Guo, M. Jia, J. Li, H. Ruan, Effect of activator/precursor mass ratio on sulfur-doped porous carbon for catalytic oxidation of aqueous organics with persulfate, Chemosphere, 303 (2022) 135–192.

[19] R. Xiao, Z. Luo, Z. Wei, S. Luo, R. Spinney, W. Yang, D. Dionysiou, Activation of peroxymonosulfate/persulfate by nanomaterials for sulfate radical-based advanced oxidation technologies, Curr. Opin. Chem. Eng., 19 (2018) 51–18.

[20] K.S. Suslick, Sonochemistry, Science, 247 (1990) 1439–1445.

[21] A. Ziylan, S. Dogan, S. Agopcan, R. Kidak, V. Aviyente, N.H. Ince, Sonochemical degradation of diclofenac: by-product assessment, reaction mechanisms, and environmental considerations, Environ. Sci. Pollut. Res., 21 (2014) 5929–5939.

[22] Z.H. Diao, F.X. Dong, L. Yan, Z.L. Chen, W. Qian, L.J. Kong, Z.W. Zhang, T. Zhang, X.Q. Tao, J.J. Du, D. Jiang, W. Chu, Synergistic oxidation of Bisphenol A in a heterogeneous ultrasound-enhanced sludge biochar catalyst/persulfate process: reactivity and mechanism, J. Hazard. Mater., 384 (2020) 121385, doi: 10.1016/j.jhazmat.2019.121385.

[23] Y.T. Li, D. Li, L.J. Lai, Y.H. Li, Remediation of petroleum hydrocarbon contaminated soil by using activated persulfate with ultrasound and ultrasound/Fe, Chemosphere, 238 (2020) 124657, doi: 10.1016/j.chemosphere.2019.124657.

[24] Q. Wang, Y. Cao, H. Zeng, Y. Liang, J. Ma, X. Lu, Ultrasound-enhanced zero-valent copper activation of persulfate for the

degradation of bisphenol AF, Chem. Eng. J., 378 (2019) 122143, doi: 10.1016/j.cej.2019.122143.
[25] S. Chakma, S. Praneeth, V.S. Moholkar, Mechanistic investigations in sono-hybrid (ultrasound/Fe^{2+}/UVC) techniques of persulfate activation for degradation of Azorubine, Ultrason. Sonochem., 38 (2017) 652–663.
[26] X. Wu, G. Xu, J.J. Zhu, Sonochemical synthesis of Fe_3O_4/carbon nanotubes using low-frequency ultrasonic devices and their performance for heterogeneous sono-persulfate process on inactivation of *Microcystis aeruginosa*, Ultrason. Sonochem., 58 (2019) 104634, doi: 10.1016/j.ultsonch.2019.104634.
[27] Y. Liu, Z. Liu, Y. Wang, Y. Yin, J. Pan, J. Zhang, Q. Wang, Simultaneous absorption of SO_2 and NO from flue gas using ultrasound/Fe^{2+}/heat coactivated persulfate system, J. Hazard. Mater., 342 (2018) 326–334.
[28] N. Yousefi, S. Pourfadakari, S. Esmaeili, A.A. Babaei, Mineralization of high saline petrochemical wastewater using sonoelectro-activated persulfate: degradation mechanisms and reaction kinetics, Microchem. J., 147 (2019) 1075–1082.
[29] Y.q. Gao, N.y. Gao, W. Wang, S.f. Kang, J.h. Xu, H.m. Xiang, D.q. Yin, Ultrasound-assisted heterogeneous activation of persulfate by nano zero-valent iron (nZVI) for the propranolol degradation in water, Ultrason. Sonochem., 49 (2018) 33–40.
[30] S.G. Babu, P. Aparna, G. Satishkumar, M. Ashokkumar, B. Neppolian, Ultrasound-assisted mineralization of organic contaminants using a recyclable $LaFeO_3$ and Fe^{3+}/persulfate Fenton-like system, Ultrason. Sonochem., 34 (2017) 924–930.
[31] F. Sepyani, R. Darvishi Cheshmeh Soltani, S. Jorfi, H. Godini, M. Safari, Implementation of continuously electro-generated Fe_3O_4 nanoparticles for activation of persulfate to decompose amoxicillin antibiotic in aquatic media: UV_{254} and ultrasound intensification, J. Environ. Manage., 224 (2018) 315–326.
[32] T. Zhang, Y. Yang, J. Gao, X. Li, H. Yu, N. Wang, P. Du, R. Yu, H. Li, X. Fan, Z. Zhou, Synergistic degradation of chloramphenicol by ultrasound-enhanced nanoscale zero-valent iron/persulfate treatment, Sep. Purif. Technol., 240 (2020) 116575, doi: 10.1016/j.seppur.2020.116575.
[33] L. Peng, L. Wang, X. Hu, P. Wu, X. Wang, C. Huang, X. Wang, D. Deng, Ultrasound-assisted, thermally activated persulfate oxidation of coal tar DNAPLs, J. Hazard. Mater., 318 (2016) 497–506.
[34] J. Guo, L. Zhu, N. Sun, Y. Lan, Degradation of nitrobenzene by sodium persulfate activated with zero-valent zinc in the presence of low-frequency ultrasound, J. Taiwan Inst. Chem. Eng., 78 (2017) 137–143.
[35] D. Deng, X. Lin, J. Ou, Z. Wang, S. Li, M. Deng, Y. Shu, Efficient chemical oxidation of high levels of soil-sorbed phenanthrene by ultrasound-induced, thermally activated persulfate, Chem. Eng. J., 265 (2015) 176–183.
[36] S. Vajnhandl, A.M. Le Marechal, Case study of the sonochemical decoloration of textile azo dye Reactive Black 5, J. Hazard. Mater., 141 (2007) 329–335.
[37] M.H. Entezari, Z.S. Al-Hoseini, N. Ashraf, Fast and efficient removal of Reactive Black 5 from aqueous solution by a combined method of ultrasound and sorption process, Ultrason. Sonochem., 15 (2008) 433–437.
[38] C. Liang, C.F. Huang, N. Mohanty, R.M. Kurakalva, A rapid spectrophotometric determination of persulfate anion in ISCO, Chemosphere, 73 (2008) 1540–1543.
[39] J. Hudzicki, Kirby-Bauer Disk Diffusion Susceptibility Test Protocol, American Society of Microbiology, 2009.
[40] R.F. Contamine, A.M. Wilhelm, J. Berlan, H. Delmas, Power measurement in sonochemistry, Ultrason. Sonochem., 2 (1995) 43–47.
[41] O.S. Arvaniti, Z. Frontistis, M.C. Nika, R. Aalizadeh, N.S. Thomaidis, D. Mantzavinos, Sonochemical degradation of trimethoprim in water matrices: effect of operating conditions, identification of transformation products and toxicity assessment, Ultrason. Sonochem., 67 (2020) 105139, doi: 10.1016/j.ultsonch.2020.105139.
[42] O.S. Arvaniti, A.A. Ioannidi, D. Mantzavinos, Z. Frontistis, Heat-activated persulfate for the degradation of micropollutants in water: a comprehensive review and future perspectives, J. Environ. Manage., 318 (2022) 155568, doi: 10.1016/j.jenvman.2022.115568.
[43] R. Kishor, D. Purchase, G.D. Saratale, L.F.R. Ferreira, M. Bilal, H.M.N. Iqbal, R.N. Bharagava, Environment-friendly degradation and detoxification of Congo red dye and textile industry wastewater by a newly isolated *Bacillus cohnni* (RKS9), Environ. Technol. Innov., 22 (2021) 101425, doi: 10.1016/j.eti.2021.101425.
[44] J. Wu, H. Zhang, J. Qiu, Degradation of Acid Orange 7 in aqueous solution by a novel electro/Fe^{2+}/peroxydisulfate process, J. Hazard. Mater., 215–216 (2012) 138–145.
[45] M.E. Bouraie, W.S.E. Din, Biodegradation of Reactive Black 5 by *Aeromonas hydrophila* strain isolated from dye-contaminated textile wastewater, Sustain. Environ. Res., 26 (2016) 209–216.
[46] R. Al-Tohamy, J. Sun, M.F. Fareed, E.-F. Kenawy, S.S. Ali, Ecofriendly biodegradation of Reactive Black 5 by newly isolated *Sterigmatomyces halophilus* SSA1575, valued for textile azo dye wastewater processing and detoxification, Sci. Rep., 10 (2020) 12370, doi: 10.1038/s41598-020-69304-4.
[47] H. Nassehinia, H. Rahmani, K. Rahmani, A. Rahmani, Solar photocatalytic degradation of Reactive Black 5: by-products, bio-toxicity, and kinetic study, Desal. Water Treat., 206 (2020) 385–395.
[48] O.A. Andrew, S. Pirgalıoğlu, Ş. Doğan, Heat activated persulfate oxidation of Reactive Black 5, Desal. Water Treat., 177 (2020) 393–399.